

# Synthesis, self-assembly, and magnetic behavior of a two-dimensional superlattice of single-crystal $\epsilon$ -Co nanoparticles

Victor F. Puentes and Kannan M. Krishnan<sup>a)</sup>

*Materials Sciences Division, Lawrence Berkeley National Laboratory, University of California, Berkeley, California 94720*

Paul Alivisatos

*Chemistry Department, University of California, Berkeley, California 94720*

(Received 9 October 2000; accepted for publication 15 February 2001)

A method of producing high-quality magnetic colloidal dispersions by the rapid pyrolysis of cobalt carbonyl in an inert atmosphere was employed to produce monodispersed, stabilized, defect-free  $\epsilon$ -cobalt nanocrystals, with spherical shapes and sizes ranging from 3 to 17 nm. The size distribution and the shape of the nanocrystals were controlled by varying the surfactant (oleic acid, phosphonic oxides and acids, etc.), its concentration, and the reaction temperature. These particles have been observed to produce two-dimensional self-assemblies when evaporated at low rates in a controlled atmosphere. A collective behavior due to dipolar interactions has been observed in the low susceptibility measurements corresponding to a highly ordered fine particles system. © 2001 American Institute of Physics. [DOI: 10.1063/1.1362333]

The development, characterization, and exploitation of novel materials based on the assembly of molecular components (nanoparticles) is an exceptionally active and rapidly expanding field. At the nanometer scale, the properties of materials can be dramatically changed when the borderline of what is called the solid state is reached. Properties arise from the large fraction of atoms which reside on the surface of the nanoparticle, and from the finite number of atoms in each crystalline core. It was in magnetic materials that such finite-size effects were recognized<sup>1</sup> with more subtle effects noted later in nonmagnetic metals such as semiconductors.<sup>2,3</sup>

We report the synthesis of monosized, nanoscale magnetic particles and their dispersion by self-assembly into two-dimensional (2D) arrays. The focus is on building solids with tailored magnetic properties and to make a breakthrough in the principal challenge facing work in low-dimension structures; i.e., how to make the transition from individual nanoscale behavior to bulk macroscopic phenomena and properties.<sup>4</sup> It has been recently shown that nanocrystals can self assemble in 2D and 3D arrays with long range translational and even orientational order. Such order can be studied at two different length scales: The atomic dimension (the crystal itself) and the nanocrystal molecular dimension (the distances between crystals or the geometry of the superlattice).<sup>5</sup> Nanocrystals can be organized into close packed arrays simply by evaporating the solvent from a hydrophobic sterically stabilized dispersion, provided that the size distribution of the particles is sufficiently narrow (i.e., a standard deviation about the mean diameter of less than 10%). Thus, these arrays may reproduce the nanoscale properties in macroscopic materials through homogeneity and periodicity, and elicit collective electronic, magnetic, and optical behavior resulting from the relative positioning of the nanocrystals in the array.<sup>3,6–8</sup>

Magnetic metal particles experience strong van der Waals attractions which, combined with their magnetic dipole interactions, makes stabilizing these systems very challenging. Different magnetic nanoparticles, such as Co,<sup>9,10</sup> CoO,<sup>11</sup> and FePt,<sup>12</sup> have been recently synthesized by solution phase metal salt reduction. Those particles may display a multiply twinned crystal structure and chemical contamination from the reducing agent. In addition, a size selective precipitation method may be required after the synthesis in order to obtain a narrow enough size dispersion (see Ref. 12 for example of self-limiting growth).

We describe a method for the production of monodisperse magnetic colloids (ferrofluids) of stabilized cobalt nanocrystals, based on the rapid pyrolysis of the organic precursor  $\text{Co}_2(\text{CO})_8$  in an inert (Ar) atmosphere and in the presence of an organic surfactant (oleic acid, lauric acid, tri-octylphosphonic acid and oxide, pyridine, etc.) at high temperatures. These conditions lead to extremely narrow size distributions, avoiding costly size selective procedures. Colloidal solutions of Co nanocrystals are stable over months, and no evidence for the formation of CoO or  $\text{Co}_3\text{O}_4$  has been observed by x-ray diffraction (XRD), transmission electron microscopy (TEM), or related spectroscopies (EDX, EELS). The surfactant, by coating the particles with a close-packed monolayer of coordinating ligand, has the ability to control the size of the growing particles; In addition, it prevents their agglomeration, passivates them against oxidation, and defines the interparticle distance in the dried samples. This synthesis was carried out using standard airless procedures and commercially available reagents.

A concentrate solution of  $\text{Co}_2(\text{CO})_8$  (0.45–0.80 g in 2–3 ml of o-dichlorobenzene anhydrous) was injected in an o-dichlorobenzene anhydrous refluxing bath (15 ml,  $T = 181^\circ\text{C}$ ). The decomposition and nucleation occurs instantaneously upon injection. The lifetime of atoms in solution is short leading to the simultaneous formation of many small metal clusters (nuclei). The surfactant is present in the hot

<sup>a)</sup>Electronic mail: krishnan@lbl.gov

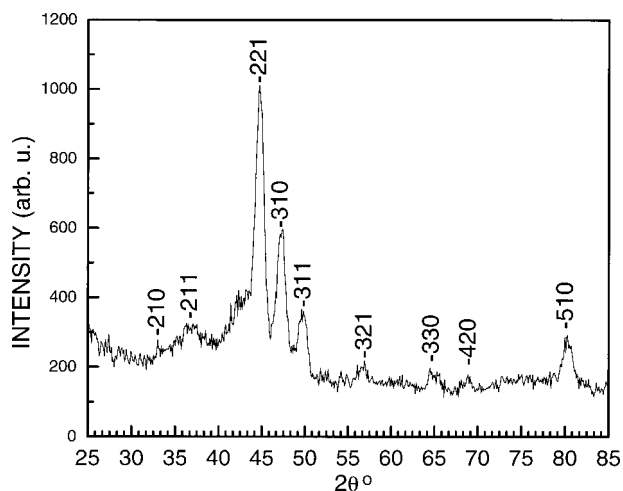


FIG. 1. XRD pattern ( $\theta$ - $2\theta$  scan) of Co nanocrystal particles. All the peaks observed can be indexed as  $\epsilon$ -Co. The peak widths confirm an average particle size of 9.1 nm.

bath at concentrations of about 1%. Mixtures of oleic acid, lauric acid, pure and technical trioctylphosphine have been used. Control of the bath temperature and the surfactant composition modifies the strength of the metallic particle-organic molecule bonding. Thus, by controlling the precursor/surfactant ratio, the reaction temperature and injection time, the size of the spherical particles can be controlled and varied between 3 and 17 nm. This method produces macroscopic quantities of Co single crystals that are monodisperse within the limit of atomic roughness. These particles are stable in air.

There are only two stable crystal phases expected for elemental Cobalt at ambient pressures (hcp below 425 °C and fcc at higher temperatures). However, in these samples, the Co particles are defect-free single crystals with a complex cubic primitive structure ( $P4_332$ ), related to the beta phase of manganese (6.20 Å in the  $\beta$ -Mn), with 20 atoms present in a cube of 6.09 Å as observed by Murray *et al.*<sup>9</sup> and called  $\epsilon$ -Co. In Fig. 1, a  $\theta$ - $2\theta$  x-ray diffraction scan for a sample of regular 10 nm spherical particles is shown. The observed peaks correspond to the following reflections obtained from the diffraction with the Cu  $K_\alpha$  radiation: (210) at 32.52°, (211) at 35.98°, (211) at 44.42°, (310) at 46.78°, (311) at 49.16°, (321) at 56.32°, (330) at 64.68°, (420) at 68.38°, (510) at 79.88°, and (520) at 86.00°. The FWHM of the peaks of Fig. 1 indicated an average crystal size of 91 Å, which roughly corresponds to the particle size observed in TEM. X-ray emission spectroscopy and electron energy-loss spectroscopy (EELS) using nanometer-scale electron probes in a TEM, confirmed that the particles are pure Co. High resolution phase contrast imaging (HREM) also show that the particles are defect-free single crystals [Fig. 2(c)]. In Fig. 2(b), we show (to our knowledge) the first diffraction patterns of a single  $\epsilon$ -Co nanocrystal using a focused electron probe that confirms the Co cubic structure. A more detailed description of the synthesis and the microstructure is to be published elsewhere.<sup>13</sup>

These particles have been observed to produce hexagonal 2D self-assemblies when evaporated at low rates in a controlled atmosphere. A drop of the resulting colloids (2% of particles in the volume) was slowly evaporated on a car-

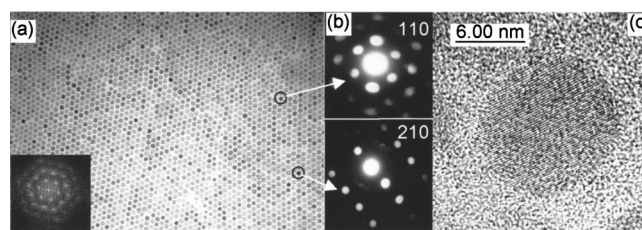


FIG. 2. (a) Bright field TEM images of a self-assembled superlattice array of mono-size (9 nm) dispersed spherical Co nanoparticles. The Fourier transform of this image (inset) confirms the perfect 2D hexagonal superlattice. (b) Electron diffraction patterns using a focused probe of 8 nm diameter from a single  $\epsilon$ -Co nanocrystal along the (110) and (210) zone axis. (c) A high-resolution phase contrast image of an  $\epsilon$ -Co nanoparticle showing it to be defect-free, spherical, and single crystalline.

bon coated TEM grid at room temperature [Fig. 2(a)]. The use of high boiling solvents allow slow evaporation at high temperature. This added thermal energy permits the particles to diffuse to their lowest energy sites during evaporation, producing a well-defined superlattice structure. The hexagonal arrangement of the nanocrystal superlattice formation is driven by surface tension, attractive van der Waals forces, and magnetic interaction among superparamagnetic particles. This assembly process is reversible by immersing the sample into alkanes. The assembly is determined by the size of the crystals and the thickness of the coating layer ( $\sim 2$  nm). No regular hexagonal assemblies have been observed in the larger particles due to the strong dipole-dipole interactions during agglomeration (suggesting that the superparamagnetic-ferromagnetic transition, at room temperature, takes place for particles of  $\sim 12$  nm diameter, as discussed shortly). Higher initial concentrations lead to 3D self assemblies where the particles in the second layer occupy sites determined by the hexagonal close-packing arrangements (not shown).

Magnetic properties of those nanoparticles have been studied from zero-field cool and field cool (ZFC/FC) curves, and from hysteresis loops at different temperatures,  $\epsilon$ -Co is a soft magnetic material that displays a magnetocrystalline anisotropy between that of fcc and hcp Co. From the hysteresis loops the anisotropy has been estimated to be  $\sim 1.5 \times 10^6$  erg/cm<sup>3</sup> at RT.<sup>14</sup> For both hcp and fcc Co, the particles are expected to be single domains<sup>15</sup> at sizes smaller than about 70 nm, thus we expect a similar limit in  $\epsilon$ -Co which has a comparable anisotropy.

The ZFC/FC curves of a 2D nanocrystal array (Fig. 2) were recorded at 50 Oe. The ZFC shows a gradual increase of the magnetization up to around 47 K, which suggest a progressive rotation of the magnetization of blocked magnetic particles towards the field direction. At 47 K the magnetization, instead of forming a peak as expected for small particles,<sup>1</sup> becomes almost constant up to RT. Between 47 and 300 K the FC curve is completely flat, suggesting a ferromagnet-like behavior. This could be explained by considering that dipolar interactions in highly ordered particles systems are magnetizing,<sup>16</sup> while in more disordered systems dipolar interactions are generally demagnetizing.<sup>17</sup> At  $T < 47$  K in the ZFC curve the system is randomly oriented and the collective behavior does not appear until 47 K, when the thermal energy is sufficiently high to let the magnetic dipoles arrange in a FM manner. From this temperature (47

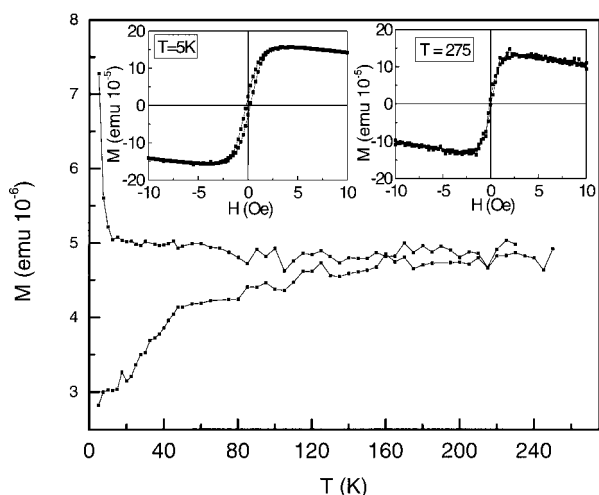


FIG. 3. ZFC/FC magnetization curves measured at 50 Oe of 9 nm  $\epsilon$ -Co particles self assembly. Insets show the magnetic hysteresis loops at 5 and 275 K.

K) a K value of  $8 \times 10^5$  erg/cm<sup>3</sup> has been estimated.<sup>1</sup> A strong paramagnetic contribution has been observed in the FC curve at very low temperatures where the magnetization increases drastically after field-cooling the sample. This is attributed to the Co-surfactant particle interface, since no magnetic atomic impurities are present in this sample. The hysteresis loops at 5 and 300 K (inset Fig. 3) show the typical features of weakly interacting superparamagnetic particles. A small hysteresis is observed at low  $T$ , and it decreases as  $T$  is increased as the thermal energy progressively overcome the interactions. At high fields ( $H > 2000$  Oe), the diamagnetic contribution of the substrate is observed in the negative slope of the magnetization curve.

The hysteresis loops at room temperature of the dried powder for different particle sizes (not shown) had the expected behavior. The smaller Co spheres (5 nm) dried sample is more difficult to magnetize (saturation field larger) than the larger (9 nm) ones. The former also displays a larger superparamagnetic contribution and a lower magnetization, both related to finite-size and surface effects which increase with decreasing sample size. In agglomerated samples (where the surfactant has been removed by heating under vacuum), bulk-like behavior is observed, as expected.

In summary, monosize-dispersed, single domain Co nanocrystals have been synthesized by chemical routes. These particles spontaneously arrange themselves in hexagonal arrays when they are slowly evaporated from a concentrated solution. Owing to the regular distribution of the dipoles in the obtained arrays, a collective behavior (very stable magnetic phase) is observed in the magnetic measurements suggesting a ferromagnetic coupling among the dipoles.

The authors would like to thank Professor Hong-Kun Park for his invaluable help at the beginning of this project. This work was supported by the U.S. DOE under Contract No. DE-AC03-76SF00098.

- <sup>1</sup>J. L. Dorman, D. Fiorani, and E. Tronc, *Adv. Chem. Phys.* **98**, 283 (1997).
- <sup>2</sup>A. P. Alivisatos, *Science* **271**, 933 (1996).
- <sup>3</sup>C. B. Murray, C. R. Kagan, and M. G. Bawendi, *Science* **270**, 1335 (1995); C. B. Murray, D. J. Norris, and M. G. Bawendi, *J. Am. Chem. Soc.* **115**, 8706 (1993).
- <sup>4</sup>G. Schmid and F. L. Chi, *Adv. Mater.* **10**, 515 (1998); A. P. Alivisatos, P. F. Barbara, A. Welford Castleman, J. Chang, D. A. Dixon, M. L. Klein, G. L. McLendon, J. S. Miller, M. A. Ratner, P. J. Rossky, S. I. Stupp, and M. E. Thompson, *Adv. Mater.* **10**, 1297 (1998); F. J. Himpsel, J. E. Ortega, G. J. Mankey, and R. F. Willis, *Adv. Phys.* **47**, 511 (1998).
- <sup>5</sup>Z. L. Wang, *Adv. Mater.* **10**, 13 (1998); P. Ohara, D. V. Leff, J. R. Heath, and W. M. Gelbart, *Phys. Rev. Lett.* **75**, 3466 (1995).
- <sup>6</sup>R. P. Andres, J. D. Bielefeld, J. I. Henderson, D. B. Janes, V. R. Kolagunta, C. P. Kubiak, W. J. Mahoney, and R. G. Osifchin, *Science* **273**, 1690 (1996).
- <sup>7</sup>S. A. Harfenist, Z. L. Wang, M. M. Alvarez, I. Vezmar, and R. L. Whetten, *J. Phys. Chem.* **100**, 13904 (1996).
- <sup>8</sup>B. A. Korgel, S. Fullam, S. Connolly, and D. Fitzmaurice, *J. Phys. Chem. B* **102**, 8379 (1998).
- <sup>9</sup>S. Sun and C. B. Murray, *J. Appl. Phys.* **85**, 4325 (1999).
- <sup>10</sup>C. Petit, A. Taleb, and P. Pileni, *J. Phys. Chem.* **103**, 1805 (1999).
- <sup>11</sup>J. S. Yin and Z. L. Wang, *Phys. Rev. Lett.* **79**, 2570 (1997).
- <sup>12</sup>S. Sun, C. B. Murray, D. Weller, L. Folks, and A. Moser, *Science* **287**, 1989 (2000).
- <sup>13</sup>V. F. Puntes, P. Alivisatos, and Kannan M. Krishnan (unpublished).
- <sup>14</sup>S. Chikazumi, *Physics of Magnetism* (Krieger, 1964).
- <sup>15</sup>D. L. Leslie-Pelecky and R. D. Rieke, *Chem. Mater.* **8**, 1770 (1996).
- <sup>16</sup>N. S. Walmsely, C. Dean, A. Hart, D. A. Parker, and R. W. Chantrell, *J. Magn. Magn. Mater.* **170**, 81 (1997); V. Franco, X. Batlle, A. Labarta, and K. O'Grady, *J. Phys. D* **33**, 609 (2000).
- <sup>17</sup>W. Luo, S. R. Nagel, T. F. Rosenbaum, and R. E. Rosenweig, *Phys. Rev. Lett.* **67**, 2721 (1991); J. L. Dorman, R. Cherkaoui, L. Spinou, M. Nogues, F. Lucari, F. D'Orazio, D. Fiorani, A. Garcia, E. Tronc, and J. P. Jolivet, *J. Magn. Magn. Mater.* **187**, L139 (1998); D. Kechrakos and K. Troidou, *Phys. Rev. B* **58**, 12169 (1998).